Elsevier Editorial System(tm) for Acta Biomaterialia
Manuscript Draft

Manuscript Number:

Title: Titanium phosphate glass microspheres for bone tissue engineering

Article Type: Full Length Article

Keywords: Phosphate glass, titanium, microspheres, bone cells, tissue engineering

Corresponding Author: Professor Jonathan C. Knowles,

Corresponding Author's Institution: University College London

First Author: Nilay J Lakhkar

Order of Authors: Nilay J Lakhkar; Jeong-Hui Park; Nicola J Mordan; Vehid Salih; Ivan B Wall; Hae-Won Kim; Scott P King; John V Hanna; Richard A Martin; Owen Addison; Fred Mosslemans; Jonathan C. Knowles

Abstract: We have demonstrated the successful production of titanium phosphate glass microspheres in the size range of approximately 10-200 μm using an inexpensive, efficient, easily scalable process and assessed their use in bone tissue engineering applications. Glasses of the following compositions were prepared by melt-quench techniques: 0.5P2O5-0.4CaO-(0.1 - x)Na2O-xTiO2 where x = 0.03, 0.05 and 0.07 mole fraction (denoted as Ti3, Ti5 and Ti7 respectively). Several characterisation studies such as density measurement, differential thermal analysis, degradation (performed using a novel time lapse imaging technique) and pH and ion release measurements revealed significant densification of the glass structure with increased incorporation of TiO2 in the glass from 3 mol% to 5 mol%, although further TiO2 incorporation up to 7 mol% did not affect the glass structure to the same extent. Cell culture studies performed using MG63 cells over a 7-day period clearly showed the ability of the microspheres to provide a stable surface for cell attachment, growth and proliferation. Taken together, the results confirm that 5 mol% TiO2 glass microspheres, on account of their relative ease of preparation and favourable biocompatibility, are worthy candidates for use as substrate materials in bone tissue engineering applications.

Titanium phosphate glass microspheres for bone tissue engineering

Nilay J. Lakhkar [a], Jeong-Hui Park [b,c], Nicola J. Mordan [a], Vehid Salih [a], Ivan B. Wall [b,d], Hae-Won Kim [b,c], Scott P. King [e], John V. Hanna [e], Richard A. Martin [f], Owen Addison [g], J.F.W. Mosselmans [h], and Jonathan C. Knowles [a,b]*

[a] Division of Biomaterials and Tissue Engineering, UCL Eastman Dental Institute, University College London, 256 Gray's Inn Road, London WC1X 8LD, UK

[b] Department of Nanobiomedical Science and WCU Research Center, Dankook University, Cheonan 330-714, Republic of Korea

[c] Institute of Tissue Regeneration Engineering, Dankook University, Cheonan 330-714, Republic of Korea

[d] Department of Biochemical Engineering, University College London, Torrington Place, London WC1E 7JE, UK

[e] Department of Physics, University of Warwick, Coventry CV4 7AL, UK

[f] School of Engineering and Applied Sciences & Aston Research Centre for Healthy Ageing, Aston University, Birmingham B4 7ET, UK

[g] Biomaterials Unit, School of Dentistry, University of Birmingham, Birmingham B4 6NN, UK

[h] Diamond Light Source, Harwell Science and Innovation Campus, Didcot, Oxfordshire OX11 0DE, UK

* Corresponding author. Tel: +44 20 3456 1189; Fax: +44 20 3456 1227. Email: j.knowles@ucl.ac.uk

Abstract

We have demonstrated the successful production of titanium phosphate glass microspheres in the size range of approximately 10–200 µm using an inexpensive, efficient, easily scalable process and assessed their use in bone tissue engineering applications. Glasses of the following compositions were prepared by melt-quench techniques: $0.5P_2O_5$–0.4CaO–(0.1 – *x*)Na_2O–*x*TiO_2 where x = 0.03, 0.05 and 0.07 mole fraction (denoted as Ti3, Ti5 and Ti7 respectively). Several characterisation studies such as density measurement, differential thermal analysis, degradation (performed using a novel time lapse imaging technique) and pH and ion release measurements revealed significant densification of the glass structure with increased incorporation of TiO_2 in the glass from 3 mol% to 5 mol%, although further TiO_2 incorporation up to 7 mol% did not affect the glass structure to the same extent. Cell culture studies performed using MG63 cells over a 7-day period clearly showed the ability of the microspheres to provide a stable surface for cell attachment, growth and proliferation. Taken together, the results confirm that 5 mol% TiO_2 glass microspheres, on account of their relative ease of preparation and favourable biocompatibility, are worthy candidates for use as substrate materials in bone tissue engineering applications.

Keywords: Titanium, phosphate glass, microsphere, bone cells, tissue engineering

1. Introduction

Titanium phosphate glasses have been widely researched for use in orthopaedic applications because of their highly favourable material properties and ability to elicit a positive bone cell response [1-4]. From a material science perspective, these glasses are of great interest because their physicochemical properties are highly tuneable, so that subtle changes in glass composition allow for major changes in glass structure and consequently in the degradation and ion release behaviour of these materials [5, 6]. Changes in titanium phosphate glass chemistry can be brought about by variations in the concentrations of the constituent oxides or the addition of small amounts of metal oxides other than TiO_2 [7-13]. The structure of the glass network has been elucidated using diverse analytical techniques such as differential thermal analysis (DTA), Raman and Fourier transform infrared (FTIR) spectroscopies, x-ray diffraction (XRD), Solid State Nuclear Magnetic Resonance (NMR), x-ray absorption spectroscopy (XAS), Ti K-edge x-ray absorption near-edge structure (XANES) and neutron/x-ray scattering [6]. The information gained from all these analyses is beneficial to biomaterials researchers who are then able to make highly informed choices regarding the specific glass composition required for specific clinical applications.

From a biological perspective, it is now well known that titanium phosphate glasses provide a surface that is quite conducive to the attachment, growth and proliferation of bone cells [14-16]. The fact that oxides of phosphorus, sodium and calcium, which constitute the major components of most phosphate glass compositions, are also found in the mineral phase of bone is a major contributing factor to the bioactivity of these glasses, particularly considering that the ions released from these glasses can exert positive effects on bone cells [17-20]. A range of *in vitro* and *in vivo* studies have been conducted on titanium phosphate glasses and highly promising results have been obtained that offer exciting possibilities for using titanium phosphate glasses in various therapeutic applications to combat bone loss [8, 13, 14, 21-23]. In order to realise viable commercial applications of these glasses, some form of glass processing is essential, for which it is necessary to develop glass processing methodologies that are efficient, cost-effective and easily scalable. However, relatively little research has

been published thus far on processing routes that would be suitable for titanium phosphate glasses. To some extent, this can be explained by the difficulties involved in processing these glasses. Glass microfibres have been commonly produced by drawing glass melt on to a rotating steel drum at high temperature. This method has been used to produce iron phosphate glass fibres that have demonstrated their efficacy in the tissue engineering of muscle cells and neuronal cells [24-27]. However, only one report in the literature exists on the use of this method to produce titanium phosphate glass fibres [28].

In this study, we propose the use of flame spheroidisation as a method to produce microspheres from melt-derived titanium phosphate glasses. Microspheres can be produced very quickly by this method since the particle residence time in the flame is of the order of milliseconds, which makes this method feasible for commercial synthesis of titanium phosphate glass microspheres for use in biomedicine, particularly as a substrate for scalable tissue engineering approaches.

2. Materials and methods

2.1. Glass manufacture: The glasses (total 3 compositions; see Table 1) were manufactured according to the methods of Abou Neel et al. [7] using stoichiometric quantities of the following precursors (all with purities of >98% and obtained from VWR-BDH, Poole, UK) without further purification: phosphorus pentoxide (P_2O_5), calcium carbonate ($CaCO_3$), sodium dihydrogen orthophosphate (NaH_2PO_4) and titanium oxide (TiO_2). After preheating at 700°C for 30 min to remove CO_2 and H_2O, the precursor mixture was then melted according to the conditions listed in Table 1. After melting for the required period, the glass was rapidly quenched by pouring on to a steel plate at room temperature and then allowed to cool overnight.

2.2. Preparation of glass microspheres: The glasses obtained from the melt quench step were broken into fragments and the fragments were crushed to form microparticles using a Retsch MM301 milling machine (Retsch, Germany). The microparticles were then passed through a flame spheroidisation apparatus to produce microspheres in the approximate size range of 10–200 μm. The flame spheroidisation apparatus comprises the following

component assemblies: (1) blow torch connected to a MAPP gas cylinder, (2) feed and (3) collectors (see Figure 1). During operation, glass microparticles placed at one end of the trough travel to the other end under the influence of vibratory forces exerted by the DC motor. At the other end, the particles pass into the flame and then travel along the flame axis (or at varying angles to the flame axis). As they pass through the flame, they undergo spheroidisation due to surface tension forces and are then collected in the glass boxes placed one after the other below the flame (Figure 1).

The microspheres from each collector were separately visualised using by light microscopy. The material present in the collector immediately below the torch outlet was discarded since it usually contained a mixture of glass microspheres along with a significant proportion of non-spherical particles; the material in the remaining glass boxes contained very few non-spherical particles, if any, and was therefore collected and stored for further studies.

2.3. Particle size distribution: For determining the particle size distribution of the obtained microspheres, the material from all four glass boxes was collected and a small quantity of the material was then added to a drop of Fractoil synthetic immersion oil (VWR, Poole, UK) placed on a microscope slide and the material was manually dispersed in the oil. A cover slip was placed on top of the slide and the slides were then imaged on an Olympus BX50 microscope (Olympus Corporation, Japan) using a CoolSNAP-Pro cf camera (Photometrics, USA). Image analysis and microsphere diameter measurements were carried out using Image-Pro Plus software (Media Cybernetics, USA).

Based on the results of the particle size distribution experiments, microspheres in the size range 63–106 µm were used in subsequent experiments involving microspheres. These microspheres were obtained by passing the feed particles through 63 µm and 106 µm sieves (Endecotts Ltd., London, UK) on a Fritsch Spartan sieve shaker (Fritsch GmbH, Germany).

2.4. Density measurements: Density measurements were carried out on the basis of Archimedes' principle using triplicate samples of glass fragments. An analytical balance (Mettler Toledo, UK) with a density measurement kit was used for this purpose. Absolute

ethanol was used instead of water as the immersion liquid since the glasses are water-soluble in nature. The following formula was used to calculate the glass density (ρ_{glass}):

$$\rho_{glass} = [M_{air}/(M_{air} - M_{ethanol})] \times \rho_{ethanol} \qquad (1)$$

where M_{air} and $M_{ethanol}$ are the masses of the sample in air and ethanol (g), respectively, and $\rho_{ethanol}$ is the density of ethanol at ambient temperature ($g.cm^{-3}$).

2.5. Differential thermal analysis: DTA studies were performed on glass microspheres using a Setaram differential thermal analyser (Setaram, France). The samples were heated from room temperature to 1000°C at a heating rate of $20°C.min^{-1}$ using air as the purge gas; an empty platinum crucible was used as a reference. The parameters measured in DTA were the glass transition temperature (T_g), crystallisation temperature (T_c) and melting temperature (T_m).

2.6. Degradation study: Degradation studies on the glass microspheres were carried out using a time lapse imaging method. Approximately 40 mg of glass microspheres was added to a cell culture flask containing 10 ml of ultrapure high-purity deionised water (resistivity = 18.2 $M\Omega.cm^{-1}$) obtained from a PURELAB UHQ-PS (Elga Labwater, Marlow, UK). Prior to the addition of microspheres and water, the bottom inner surface of the flask had been scraped with a brush in order to provide surface roughness so that the microspheres would remain reasonably stationary during the experiment. The flask was then placed on the stage of a Leica DMIRB microscope (Leica Microsystems CMS GmbH, Germany) fitted with a Solent Scientific incubator system (Solent Scientific Ltd., Segensworth, UK). Time lapse images of the microspheres were acquired at intervals of 1 hour over an 80-hour period using a Tucsen TCA-10.0-N camera (Tucsen Image Technology Inc., China) running on µManager microscopy open source software (Ron Vale Lab, University of California San Francisco, USA); subsequent image analysis and diameter measurements were carried out using ImageJ [29]. For each glass composition, the diameters of six spheres were measured and the mass of the sphere was obtained by the equation

$$m_{sphere} = \rho_{glass} \times v_{sphere} = \rho_{glass} \times 4/3 \times \pi(r_{sphere})^3 \qquad (2)$$

where m_{sphere} is the mass of the sphere (μg); ρ_{glass}, the density of the glass obtained from the previous density measurement (μg.μm^{-3}); v_{sphere}, the volume of the sphere (μm^3); and r_{sphere}, the radius of the sphere (μm).

The percentage weight loss per unit surface area of the sphere at each time point was then calculated by the following equation:

$$[(m_{sphere(0)} - m_{sphere(t)})/m_{sphere(0)}A_t] \times 100 \qquad (3)$$

where $m_{sphere(0)}$ is the mass of the microsphere at time t = 0 (μg); $m_{sphere(t)}$, the mass of the microsphere at time t (μg); and A_t, the surface area of the microsphere at time t (μm^2).

2.7. pH and ion release measurements: The pH and ion release measurements were carried out in triplicate at the following time points: 0, 24, 72, 168, 336 and 504 hours. Prior to the measurements, approximately 250 mg of microspheres were placed in closed plastic containers containing 25 ml of deionised water. The pH of this deionised water had been previously adjusted to 7 ± 0.1 using NH_4OH or HCl. At the above time points, the solution from each container was removed and stored while the microspheres were dried and reintroduced into fresh medium. The pH of the solution was measured using an Orion pH meter (Orion, UK) that was fitted with a pH glass electrode (BDH, UK). The cation and anion release measurements were carried out by ion chromatography techniques [8]. The release of polyphosphate anions from the glass discs was analysed using a Dionex ICS-2500 ion chromatography system (Dionex, Surrey, UK) without prior purification, while Na^+ and Ca^{2+} cation release were measured using a Dionex ICS-1000 ion chromatography system after passing the solution through a Dionex OnGuard IIA cartridge to eliminate anions that bind to the cation column.

2.8. X-ray diffraction: XRD analysis was performed using methods similar to those used in a previous study [8] on microsphere samples placed in simulated biological fluid (SBF) at 37°C. For preparation of SBF, the protocol provided by Kokubo and Takadama was followed [30]. The samples were analysed on a Bruker D8 Advance Diffractometer (Bruker, UK) in flat plate geometry using Ni-filtered Cu *K*α radiation. Data was collected at 2θ values from 10° to 100° with a step size of 0.02° and a count time of 12 s. Sample analysis was first carried out

before immersing the microsphere sample in the medium (i.e. at day 0), and at time points of 3, 7 and 14 days post immersion, the microspheres were removed from the medium, dried and then analysed.

2.9. Nuclear magnetic resonance: Solid state ^{31}P magic angle spinning (MAS) NMR experiments were undertaken at 9.4 T using a Bruker DSX-400 spectrometer operating at a Larmor frequency of 161.92 MHz. All measurements were facilitated using a Bruker 4 mm dual channel probe in which MAS frequencies of 12.5 kHz were implemented. All ^{31}P MAS NMR data were acquired using single pulse experiments, where pulses of 2.5 μs duration (corresponding to π/4 flip angles) were employed with recycle delays of 240 s to achieve a quantitative survey of the P speciation. ^{31}P chemical shifts were referenced against the primary IUPAC standard of 85% H_3PO_4 (δ 0.0 ppm) via a secondary solid reference of $(NH_4)[H_2PO_4]$ (δ 1.0 ppm). Each spectrum was processed with Bruker TOPSPIN software, with the spectral deconvolutions performed using the DmFit software package [31].

2.10. Ti K-edge X-ray near edge absorption: The Ti K-edge XANES data were collected in fluorescence mode using the micro-focus beam-line I18 at the Diamond Light Source, UK. Spectra were collected from 80 eV below the edge to 220 eV above the edge in order to allow an accurate background subtraction. The spectra were collected in three step sizes; a 5-eV step size was used for the pre-edge (4900–4940 eV), a 0.25-eV step size was used over the pre-peak and edge (4940–5000 eV) and a 2-eV step size was used after the edge (5000–5200 eV). All measurements were conducted at room temperature. The spectra were normalized to have an edge step of one.

2.11. Cell culture: Cell culture studies were conducted on the basis of Chen et al.'s methods using MG63 osteoblast-type cells [32]. For seeding of cells on the glass microspheres, approximately 40 mg of glass microspheres were weighed and placed in small glass vials for sterilisation under dry heat at a temperature of 180°C for 1 hour. The microspheres were then carefully transferred to Transwell® cell culture inserts (Corning, USA) placed in 24-well plates such that the entire surface of the insert mesh was covered by a thin layer of microspheres. Subsequently, the MG63 cells were seeded on the microspheres at a seeding

density of 10,000 cells per well followed by incubation at 37°C in an atmosphere of 95% air and 5% CO_2.

Scanning electron microscopy (SEM) images were obtained at 7 days post seeding. Fixation in 3% glutaraldehyde, dehydration through a graded series of ethanol (50, 70, 90, and 100%) and drying in hexamethyldisilazane (Aldrich, UK) were carried out *in situ* in the inserts, after which each insert was taken out of the well and the entire insert mesh was carefully cut out from the insert along the edge using a scalpel. The meshes with the cell-cultured spheres on them were mounted onto aluminium stubs. The mounted samples were sputter-coated with gold/palladium and observed with a scanning electron microscope (model JSM 5410LV, JEOL, Japan) using various magnifications at an operating voltage of 10 kV.

Scanning laser confocal microscopy (SLCM) images were also obtained at 7 days after seeding using Alexa Flour 488 phalloidin (Invitrogen, UK) to stain the actin filaments of the cytoskeleton and propidium iodide (BD Biosciences, UK) to stain the nucleus. Prior to imaging, the samples were processed by first fixing in 4% paraformaldehyde until required for imaging. The fixed samples were then washed twice with phosphate buffered saline (PBS) and permeabilised using a solution of 0.1 vol% Triton-X in PBS for 3–5 min. A solution of 2.5 vol% phalloidin methanolic stock solution in PBS was then added to each sample well and the samples were maintained for 20 min in a dark atmosphere to minimise evaporation and photobleaching. After washing again with PBS, the samples were counterstained with 1 µg/ml of propidium iodide for 10 min. The stained samples were visualised by confocal microscopy (Biorad, USA).

The cell proliferation assay was conducted after 1, 4 and 7 days in culture. The control comprised the mesh of the cell culture insert with cells seeded on it. The MG63 cells were seeded on the glass microspheres and control mesh at a seeding density of 10,000 cells per well, followed by incubation at 37°C in an atmosphere of 95% air and 5% CO_2. Cell proliferation at each time point was determined using the AlamarBlue™ assay (AbD Serotec, UK) as described previously [32]. Fluorescence detection was accomplished by means of a

Fluoroskan fluorimeter (Thermo Scientific, UK) with absorption and emission values set to 530 nm and 590 nm, respectively. The fluorimeter provided absorbance data, so to plot the data in terms of the number of cells, a standard calibration curve was measured separately. For the standard curve, cell populations of 0, 10000, 20000, 50000 and 100000 cells were cultured over a 1-day period in a 24-well plate and fluorescence measurements were carried out using the same fluorimeter.

3. Results

3.1. Particle size distribution: Glass microspheres were successfully obtained for all the glass compositions over an approximate size range of between 10 µm and 200 µm (Figure 2). For all the compositions, up to 85% of the microspheres had sizes of 120 µm or less. There was no significant difference between the particle size distributions for the different glass compositions, thereby indicating that the microsphere production process was independent of the glass composition and therefore influenced by the parameters of the flame spheroidisation process, e.g. flame temperature and particle residence time in the flame.

The results obtained from the particle size distribution were further confirmed by light microscopy images of the microspheres obtained for particles of different size fractions. Taking the Ti7 microspheres as a representative example, it was observed that at particle sizes of 45–63 µm, very few microspheres were obtained (Figure 3). The feed particles tended to aggregate together on the feed trough and it was difficult to ensure adequate particle separation on the trough before the particles entered the flame; inside the flame, the particle aggregates tended to break up into the constituent particles without significant microsphere formation. At particle sizes of 106–150 µm, a significant number of particles were too large and the particle residence time in the flame was too short for the particles to undergo spheroidisation; consequently, microsphere samples in this size range tended to contain large numbers of non-spherical particles. The proportion of non-spherical particles was minimal at particle sizes of 63–75 and 75–106 µm. Therefore, in all subsequent experiments involving microspheres, a size range of 63–106 µm was adopted.

3.2. Density measurements: The density of the investigated glass compositions increased with the Ti content from 2.635 ± 0.004 g/cm^3 for Ti3 to 2.672 ± 0.002 g/cm^3 for Ti7 (Table 1). The results indicated significant structural densification with the increase in the TiO_2 content of the glass.

3.3. Differential thermal analysis: The density results were further confirmed by the increase in the T_g value of the glass from 489°C for Ti3 to 529°C for Ti7 (see Table 1 for T_g, T_c and T_m values). In all the glass compositions, two overlapping crystallisation peaks were observed, with the extent of overlap being greater for Ti3 than for Ti5 and Ti7. As with the T_g values, the T_c values for the first crystallisation peak increased with the Ti content from 689°C for Ti3 to 739°C for Ti7. All three compositions showed a single broad melting peak with T_m values ranging from 878°C for Ti3 to approximately 904–905°C for Ti5 and Ti7.

3.4. Degradation study: Figure 4 shows the percentage cumulative weight loss per unit surface area of the microspheres as a function of the degradation time for the investigated titanium phosphate glass microspheres. The plot shows that the degradation rate of the microspheres appeared to increase with time. With regard to Ti3 and Ti5, a clear correlation between the TiO_2 content and the degradation rate was observed, whereby as the TiO_2 content increased, the degradation rate of the glass microspheres decreased. At 80 hours, the percentage cumulative weight loss per unit surface area was 0.0092 %.μm^{-2} for Ti3 which was approximately 3 times that for Ti5 (0.0032 %.μm^{-2}). However, the difference between the weight loss values of the Ti5 and Ti7 microspheres was not as marked (0.0032 %.μm^{-2} for Ti5 versus 0.0024 %.μm^{-2} for Ti7). Thus, while the trend in the degradation rate at 80 hours could be represented as Ti3 > Ti5 > Ti7, the effect of TiO_2 addition on the degradation rate was appreciable only when the TiO_2 content was increased from 3 to 5 mol%. It is worth noting that the error bars of all the data points in the graph were small, which indicated the reliability of the methodology.

3.5. pH measurements: Microspheres of all the investigated glass compositions caused a decrease in pH when immersed in deionised water over the 21-day study period (Figure 5). A significantly strong decrease in pH was observed from day 0 to day 1; however, the pH

decrease became progressively more gradual over the rest of the immersion time. The measured pH values ranged from 2.8–4.5 for Ti3 to 3.4–5.5 for Ti5 and Ti7. Thus, the deionised water solution containing Ti3 microspheres was more acidic than those containing Ti5 and Ti7 microspheres. The pH trend was broadly similar to the trend observed in the degradation rate; thus, while Ti3 showed a greater pH decrease than Ti5, the pH decrease shown by Ti5 and Ti7 was not significantly different. The decrease in pH for all the glasses was attributed to the release of phosphate ions which formed phosphoric acid in the solution.

3.6. Ion release measurements: As in the degradation study, the ion release studies revealed an increase in the release of all the measured ionic species with time over the entire study period. The rates of ion release shown in Figure 6 for the Ca^{2+} ions and in Table 2 for the remaining ions are obtained by calculating the slope of the linear fit of ion release over time. For both cationic (Na^{+} and Ca^{2+}) and anionic (PO_4^{3-}, $P_3O_9^{3-}$, $P_2O_7^{4-}$ and $P_3O_{10}^{5-}$) sets of species, the ion release of Ti3 was significantly greater than that of Ti5 which in turn was greater than that of Ti7 but by a much lesser degree (Table 2).

3.7. X-ray diffraction: As shown in Figure 7 for Ti5, no apatite formation could be discerned as evidenced by the lack of crystalline peaks in the XRD spectra at all the specified time points. Similar results were obtained for Ti3 and Ti7 (data not shown).

3.8. Nuclear magnetic resonance: The ^{31}P NMR MAS spectra revealed that with increasing TiO_2 incorporation, no apparent significant change in *Q* species could be observed, although there was a monotonic upfield movement of both Q^1 and Q^2 chemical shifts towards more negative values (see Table 1), and a concomitant increase in the line widths of both Q^1 and Q^2 resonances. As a result, the Q^2/Q^1 ratio remained essentially constant for all three compositions.

3.9. Ti K-edge X-ray near edge absorption: The Ti K-edge XANES spectra (not shown) revealed that the pre-edge, for all of the samples, consisted of two small peaks at 4968 and 4970 eV with normalized intensities of 0.08 and 0.05, respectively. These results are consistent with Ti occupying a six-fold coordinated (TiO_6) environment.

3.10. Scanning electron microscopy and confocal microscopy: The SEM images (Figure 8) and SLCM images (Figure 9) results reveal that by day 7, microspheres of all the compositions were covered with a significant number of cells. Most of the microspheres appeared to be covered with a finite countable number of cells that enveloped the microsphere surface. The majority of the cells covering the spheres showed a flattened morphology. In many cases, cells on different microspheres appeared to bridge across to each other by means of cell processes. Thus, the investigated titanium phosphate glass microspheres clearly supported osteoblatic cell attachment and proliferation on their surface.

3.11. Cell proliferation assay: Cell proliferation using the AlamarBlue™ cell proliferation assay was determined over time points of 1, 4 and 7 days on the investigated titanium phosphate glass microspheres (Figure 10). The results revealed that for all the compositions studied, MG63 cells were capable of sustained expansion over the culture period. At day 1, the cell numbers for microspheres of all the compositions were similar to those on the control. On day 4, the Ti-containing phosphate glass microspheres showed comparable cell numbers, while, as expected, that of the mesh insert control was noticeably higher. By day 7, a considerable increase in cell number in comparison with days 1 and 4 was observed for all three compositions, thereby confirming not only the biocompatibility of the investigated microspheres with respect to favourable cell attachment, but also suitability as a substrate that actively supports osteoblastic cell proliferation.

4. Discussion

The present study is the first to demonstrate the successful production of melt derived phosphate glass microspheres. Several interesting results from this study suggest that the produced glass microspheres possess favourable properties and biocompatibility for use in biomedical applications.

The particle size distribution experiment was carried out to investigate whether the glass composition can affect the size of microspheres obtained from the flame spheroidisation apparatus. The microsphere size was found to be independent of the glass composition; this is a favourable result since it implies that a wider range of microsphere sizes can be

obtained by suitably modifying the flame spheroidisation set up. The present set up yielded microspheres in the size range of ~10–210 μm. At the lower end of this range, particle agglomeration in the feed apparatus and subsequent dispersal of the agglomerates in the flame considerably restricted the number of glass microspheres with sizes of <30 μm. This problem can possibly be overcome by dispersing the feed particles in a suitable liquid dispersant prior to introduction in the flame. On the other hand, at the upper end of the range, microsphere numbers were limited because the residence time of the particles in the flame was inadequate for achieving complete spheroidisation. This problem can be resolved by generating a flame of greater length and higher temperature to provide a longer residence under hotter conditions. A larger blow torch connected to a gas–oxygen source may be used for this purpose, as has been implemented in several previous glass microsphere studies [33-35]. As such, the flame spheroidisation apparatus used in the present study was found to yield maximum proportion of spherical particles over a size range of 63–105 μm; as a result, all microsphere-related experiments were conducted using spheres within this size range.

The characterisation studies yielded several sets of closely related results that clearly demonstrate the increased densification of the glass structure with the incorporation of increasing amounts of TiO_2, especially from 3 mol% to 5 mol% TiO_2. Thus, the increase in density from Ti3 to Ti5 was observed in conjunction with the increase in T_g and T_c values in the DTA and the decrease in the degradation rate, pH and ion release. It has already been explained that the increase in structural densification is associated with the formation of TiO_5 and TiO_6 units that enter the glass structure to form P–O–Ti bonds; at the same time, more Q^1 units are introduced at the expense of Q^2 units [9]. Between Ti5 and Ti7, however, the differences in degradation, pH and ion release were not as pronounced. It is possible that the addition of 5 mol% TiO_2 to the glass serves to saturate the glass structure, and any further TiO_2 that may be added has a reduced effect on the glass network. Any evidence of secondary phases is lacking as these would show evidence of 4- and 5-fold coordination.

The characterisation results are broadly in agreement with those of previous studies on TiO_2-containing quaternary phosphate glasses [2, 3, 7-9, 11, 36]. Yet, there are some

important differences that merit further discussion. Differences exist between the DTA profiles of the present study and those obtained in the previous study by Abou Neel et al. [9], particularly in terms of the presence of additional crystallisation or melting peaks. These differences may be dependent on the particle sizes of the samples being analysed. The present study utilised glass microspheres in the size range 63–106 μm, whereas it is probable that powdered samples containing particles of smaller sizes were used for DTA analyses in the previous study. The differences in the particle sizes may have preferentially promoted surface nucleated phases during the course of the experiment.

An important difference is noted between the shape of the degradation profiles in the present study and that in previous studies on TiO_2-containing phosphate glass [7-9, 11]. In previous studies, degradation experiments were conducted on glass discs and the results showed either quite linear degradation or higher degradation rates at the beginning of the experiment followed by lower rates as time progresses, leading to an overall plateau-like profile shape. On the other hand, the present study investigated the degradation of spheres and the results revealed an exponential curve. Here, it is worth noting that to the best of our knowledge, the use of a time lapse imaging technique to obtain degradation data for glass microspheres has not been reported previously; thus, this novel technique allows us to understand more accurately how glass microspheres degrade when immersed in a liquid. The degradation profile obtained in the present study has important implications for the development of microsphere-based biomedical applications, since degradation of the microspheres *in vivo* would be considered to follow a similar profile. For equivalent weights of glass microsphere and glass disc samples, the microsphere samples would possess a much larger surface area, which would lead to differences in degradation rates as well as in the local environments of the samples undergoing degradation.

The NMR and XANES results reveal very little change in either the *Q* speciation or in the Ti coordination in all three compositions. The reason for this lack of change particularly for TiO_2 contents of 7 mol% is connected to these glasses being in the metaphosphate region [37]. With regard to the XANES results, previous studies have shown that the relative height of

the pre-peak is ~0.9(1) for 4-fold Ti and ~0.4 to 0.7 for 5-fold Ti [38]. The absence of this sharp pre-edge feature at ~4970 eV therefore excludes the possibility of a significant proportion of Ti occupying either a 4- or 5-fold coordinated environment in the investigated compositions.

With regard to the XRD results, the absence of an apatite layer on the surface of the titanium phosphate glass microspheres as revealed by XRD experiments is an interesting and important result. Immersion of the biomaterial under investigation in SBF for specific time periods has been used frequently in previous studies in order to confirm the biocompatibility of the material, but it has also been argued that the lack of apatite-forming ability need not necessarily imply lack of bioactivity [6, 30]. The XRD results in this study are in agreement with those of previous studies on titanium phosphate glasses which have shown the absence of apatite formation on the glass surface upon SBF immersion even as the glasses have demonstrated a high level of bioactivity from both *in vitro* and *in vivo* tests [7-9, 14]. Furthermore, the absence of an apatite layer on the microsphere surface may even have beneficial effects on cell attachment and proliferation on account of the absence of debris formation, which allows the microspheres to offer a stable surface for cell growth. This is an important factor if developing the beads for stem cell scale up as it offers a clean methodology for expansion.

Promising results have been obtained from the cell culture experiments on the titanium phosphate glass microspheres. Both SEM and SLCM images show the attachment and spreading of MG63 osteoblastic cells on the surface of the microspheres by day 7, indicating the favourable biocompatibility of the microspheres. Furthermore, the AlamarBlue^{TM} results provide quantitative confirmation of the ability of the microspheres to provide a stable substrate for osteoblastic cell proliferation. The mesh insert control exhibits superior cell proliferation than microspheres of all compositions on day 4 and particularly on day 7, but this is to be expected, as, like tissue culture plastics, the mesh insert has been specifically developed to be highly biocompatible for multiple cell types. Specifically they are specially designed to facilitate high levels of cell attachment, growth and migration. Taking these

factors into consideration, a more suitable control for this study would be commercially available silica glass microspheres of sizes similar to those of the phosphate glass microspheres.

5. Conclusions

In summary, this study demonstrates the successful production of titanium phosphate glass microspheres in the size range of approximately 10–200 μm from glasses of compositions $0.5P_2O_5$–0.4CaO–(0.1 – *x*)Na_2O–*x*TiO_2 where x = 0.03, 0.05 and 0.07 mole fraction. The flame spheroidisation process used for this purpose is inexpensive, efficient and easily scalable, all of which are highly desirable attributes from the viewpoint of developing viable commercial applications. Glass characterisation studies show that increasing the glass TiO_2 content from 3 mol% to 5 mol% results in significant structural densification but further increase in the TiO_2 content to 7 mol% does not change the glass properties to the same extent. Cell culture studies reveal that microspheres of all the investigated compositions provide a surface that is conducive to the attachment, growth and proliferation of MG63 cells, with significant increase in cell numbers observed over a 7-day culture period. Considering the relative ease of production of 5 mol% TiO_2 glass microspheres (particularly in comparison with those containing 7 mol% TiO_2 in terms of melting time and temperature) and their optimal properties with respect to degradation, ion release and biocompatibility, we plan to use the 5 mol% TiO_2 microspheres to explore the development of clinical applications in the orthopaedic domain.

Work is now underway on the primary end application of the investigated titanium phosphate glass microspheres as a bioreactor substrate for the scale up and possible guided differentiation of human mesenchymal stem cells (hMSCs). Bioreactors offer dynamic 3D *in vitro* environments that can closely mimic *in vivo* conditions and are therefore an important tool not only for the *in vitro* growth of tissue substitutes, which is indeed the goal of all tissue engineering approaches, but also for researching the responses of cells and tissues to various stimuli of mechanical and biochemical origin. It is envisaged that two types of bioreactors might be used in order to develop viable bone tissue from hMSCs. Initial cell

growth will be carried out in spinner flasks, after which it will be necessary to further culture the cells in perfusion bioreactor systems in order to ensure proper tissue growth and encourage cell differentiation. It is anticipated that the end product of these approaches will be the development of viable small-sized bone tissue that can be used for the treatment of bone loss caused by congenital abnormalities, traumatic injuries or disease.

Acknowledgements

This work was supported by WCU Program through the National Research Foundation of Korea (NRF) funded by the Ministry of Education, Science and Technology (No. R31-10069). The UCL Graduate School is thanked for the GRS and ORS scholarships provided for NJL. JVH thanks EPSRC and the University of Warwick for partial funding of the solid state NMR infrastructure at Warwick, and acknowledges additional support for this infrastructure obtained through Birmingham Science City: Innovative Uses for Advanced Materials in the Modern World (West Midlands Centre for Advanced Materials Project 1), with support from Advantage West Midlands (AWM) and partial funding by the European Regional Development Fund (ERDF). This work was carried out with the support of Diamond Light Source. JVH thanks EPSRC and the University of Warwick for partial funding of the solid state NMR infrastructure at Warwick, and acknowledges additional support for this infrastructure obtained through Birmingham Science City: Innovative Uses for Advanced Materials in the Modern World (West Midlands Centre for Advanced Materials Project 1), with support from Advantage West Midlands (AWM) and partial funding by the European Regional Development Fund (ERDF).

References

[1] Navarro M, Ginebra MP, Planell JA. Cellular response to calcium phosphate glasses with controlled solubility. Journal of Biomedical Materials Research Part A 2003;67A:1009-15.
[2] Navarro M, Ginebra MP, Clement J, Martinez S, Avila G, Planell JA. Physicochemical degradation of titania-stabilized soluble phosphate glasses for medical applications. Journal of the American Ceramic Society 2003;86:1345-52.
[3] Rajendran V, Devi AVG, Azooz M, El-Batal FH. Physicochemical studies of phosphate based P2O5-Na2O-CaO-TiO2 glasses for biomedical applications. J Non-Cryst Solids 2007;353:77-84.
[4] Vitale-Brovarone C, Ciapetti G, Leonardi E, Baldini N, Bretcanu O, Verne E, et al. Resorbable Glass-Ceramic Phosphate-based Scaffolds for Bone Tissue Engineering: Synthesis, Properties, and In vitro Effects on Human Marrow Stromal Cells. J Biomater Appl 2011;26:465-89.
[5] Abou Neel EA, Pickup DM, Valappil SP, Newport RJ, Knowles JC. Bioactive functional materials: a perspective on phosphate-based glasses. Journal of Materials Chemistry 2009;19:690-701.
[6] Kiani A, Lakhkar NJ, Salih V, Smith ME, Hanna JV, Newport RJ, et al. Titanium-containing bioactive phosphate glasses. Philos T R Soc A 2012;370:1352-75.
[7] Abou Neel EA, Chrzanowski W, Knowles JC. Effect of increasing titanium dioxide content on bulk and surface properties of phosphate-based glasses. Acta Biomater 2008;4:523-34.
[8] Abou Neel EA, Knowles JC. Physical and biocompatibility studies of novel titanium dioxide doped phosphate-based glasses for bone tissue engineering applications. Journal of Materials Science-Materials in Medicine 2008;19:377-86.
[9] Abou Neel EA, Chrzanowski W, Valappil SP, O'Dell LA, Pickup DM, Smith ME, et al. Doping of a high calcium oxide metaphosphate glass with titanium dioxide. J Non-Cryst Solids 2009;355:991-1000.
[10] Abou Neel EA, O'Dell LA, Chrzanowski W, Smith ME, Knowles JC. Control of Surface Free Energy in Titanium Doped Phosphate Based Glasses by Co-Doping With Zinc. Journal of Biomedical Materials Research Part B-Applied Biomaterials 2009;89B:392-407.
[11] Kiani A, Cahill LS, Abou Neel EA, Hanna JV, Smith ME, Knowles JC. Physical properties and MAS-NMR studies of titanium phosphate-based glasses. Materials Chemistry and Physics 2010;120:68-74.
[12] Moss RM, Abou Neel EA, Pickup DM, Twyman HL, Martin RA, Henson MD, et al. The effect of zinc and titanium on the structure of calcium-sodium phosphate based glass. J Non-Cryst Solids 2010;356:1319-24.
[13] Lakhkar N, Abou Neel EA, Salih V, Knowles JC. Titanium and Strontium-doped Phosphate Glasses as Vehicles for Strontium Ion Delivery to Cells. Journal of biomaterials applications 2010.
[14] Abou Neel EA, Mizoguchi T, Ito M, Bitar M, Salih V, Knowles JC. In vitro bioactivity and gene expression by cells cultured on titanium dioxide doped phosphate-based glasses. Biomaterials 2007;28:2967-77.
[15] Del Valle LJ, Navarro M, Sepulcre F, Ginebra MP, Planell JA. Growth and differentiation of osteogenic cells on calcium phosphate glasses. European Biophysics Journal 2003;32:269.
[16] Brauer DS, Russel C, Li W, Habelitz S. Effect of degradation rates of resorbable phosphate invert glasses on in vitro osteoblast proliferation. Journal of Biomedical Materials Research Part A 2006;77A:213-9.
[17] Knowles JC. Phosphate based glasses for biomedical applications. Journal of Materials Chemistry 2003;13:2395-401.
[18] Blair HC, Schlesinger PH, Huang CL, Zaidi M. Calcium signalling and calcium transport in bone disease. Sub-cellular biochemistry 2007;45:539-62.
[19] Riddle RC, Taylor AF, Genetos DC, Donahue HJ. MAP kinase and calcium signaling mediate fluid flow-induced human mesenchymal stem cell proliferation. American journal of physiology Cell physiology 2006;290:C776-84.

[20] Foster BL, Tompkins KA, Rutherford RB, Zhang H, Chu EY, Fong H, et al. Phosphate: known and potential roles during development and regeneration of teeth and supporting structures. Birth defects research Part C, Embryo today : reviews 2008;84:281-314.
[21] Lakhkar NJ, Abou Neel EA, Salih V, Knowles JC. Strontium oxide doped quaternary glasses: effect on structure, degradation and cytocompatibility. Journal of Materials Science-Materials in Medicine 2009;20:1339-46.
[22] Dias AG, Lopes MA, Santos JD, Afonso A, Tsuru K, Osaka A, et al. In vivo performance of biodegradable calcium phosphate glass ceramics using the rabbit model: Histological and SEM observation. Journal of biomaterials applications 2006;20:253-66.
[23] Monem AS, ElBatal HA, Khalil EMA, Azooz MA, Hamdy YM. In vivo behavior of bioactive phosphate glass-ceramics from the system P2O5-Na2O-CaO containing TiO2. Journal of Materials Science-Materials in Medicine 2008;19:1097-108.
[24] Ahmed I, Collins CA, Lewis MP, Olsen I, Knowles JC. Processing, characterisation and biocompatibility of iron-phosphate glass fibres for tissue engineering. Biomaterials 2004;25:3223-32.
[25] Abou Neel EA, Ahmed I, Blaker JJ, Bismarck A, Boccaccini AR, Lewis MP, et al. Effect of iron on the surface, degradation and ion release properties of phosphate-based glass fibres. Acta Biomater 2005;1:553-63.
[26] Shah R, Sinanan ACM, Knowles JC, Hunt NP, Lewis MP. Craniofacial muscle engineering using a 3-dimensional phosphate glass fibre construct. Biomaterials 2005;26:1497-505.
[27] Alekseeva T, Abou Neel EA, Knowles JC, Brown RA. Development of Conical Soluble Phosphate Glass Fibers for Directional Tissue Growth. J Biomater Appl 2012;26:733-44.
[28] Vitale-Brovarone C, Novajra G, Milanese D, Lousteau J, Knowles JC. Novel phosphate glasses with different amounts of TiO2 for biomedical applications Dissolution tests and proof of concept of fibre drawing. Materials Science & Engineering C-Materials for Biological Applications 2011;31:434-42.
[29] Abramoff MD, Magalhaes PJ, Ram SJ. Image Processing With ImageJ. Biophotonics International 2004;11:36-42.
[30] Kokubo T, Takadama H. How useful is SBF in predicting in vivo bone bioactivity? Biomaterials 2006;27:2907-15.
[31] Massiot D, Fayon F, Capron M, King I, Le Calve S, Alonso B, et al. Modelling one- and two-dimensional solid-state NMR spectra. Magn Reson Chem 2002;40:70-6.
[32] Chen QZ, Efthymiou A, Salih V, Boccaccini AR. Bioglass-derived glass-ceramic scaffolds: study of cell proliferation and scaffold degradation in vitro. Journal of biomedical materials research Part A 2008;84:1049-60.
[33] Cacaina D, Ylanen H, Simon S, Hupa M. The behaviour of selected yttrium containing bioactive glass microspheres in simulated body environments. Journal of Materials Science-Materials in Medicine 2008;19:1225-33.
[34] Sene FF, Okuno E, Martinelli JR. Synthesis and characterization of phosphate glass microspheres for radiotherapy applications. J Non-Cryst Solids 2008;354:4887-93.
[35] Martinelli JR, Sene FF, Kamikawachi CN, Partiti CSD, Cornejo DR. Synthesis and characterization of glass-ceramic microspheres for thermotherapy. J Non-Cryst Solids 2010;356:2683-8.
[36] Pickup DM, Abou Neel EA, Moss RM, Wetherall KM, Guerry P, Smith ME, et al. TiK-edge XANES study of the local environment of titanium in bioresorbable TiO2-CaO-Na2O-P2O5 glasses. Journal of Materials Science-Materials in Medicine 2008;19:1681-5.
[37] Brow RK. Review: the structure of simple phosphate glasses. J Non-Cryst Solids 2000;263:1-28.
[38] Farges F, Brown GE, Rehr JJ. Coordination chemistry of Ti(IV) in silicate glasses and melts .1. XAFS study of titanium coordination in oxide model compounds. Geochim Cosmochim Ac 1996;60:3023-38.

Figure 1
Click here to download high resolution image

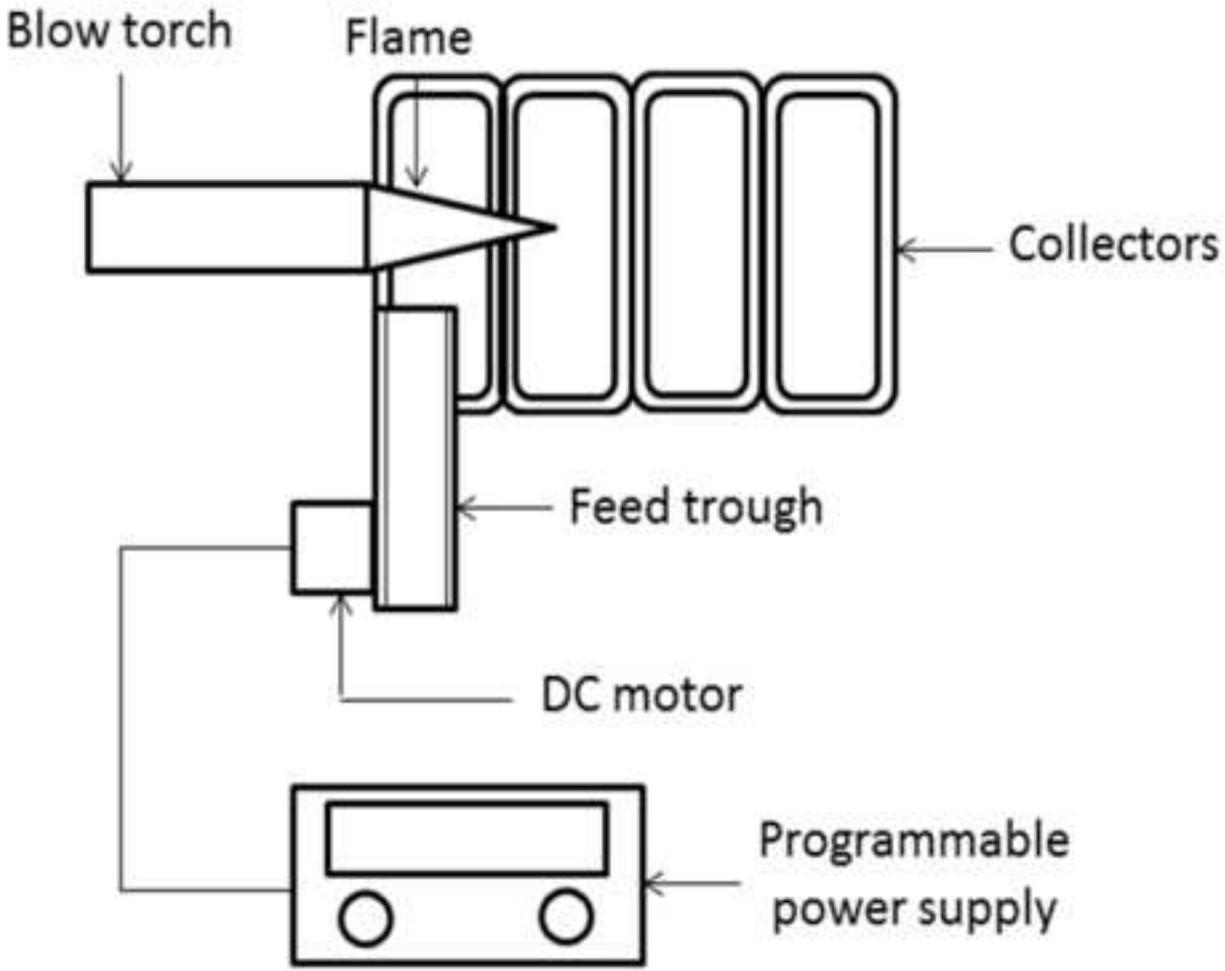

Figure 1: Schematic diagram of flame spheroidisation apparatus

Figure 2
Click here to download high resolution image

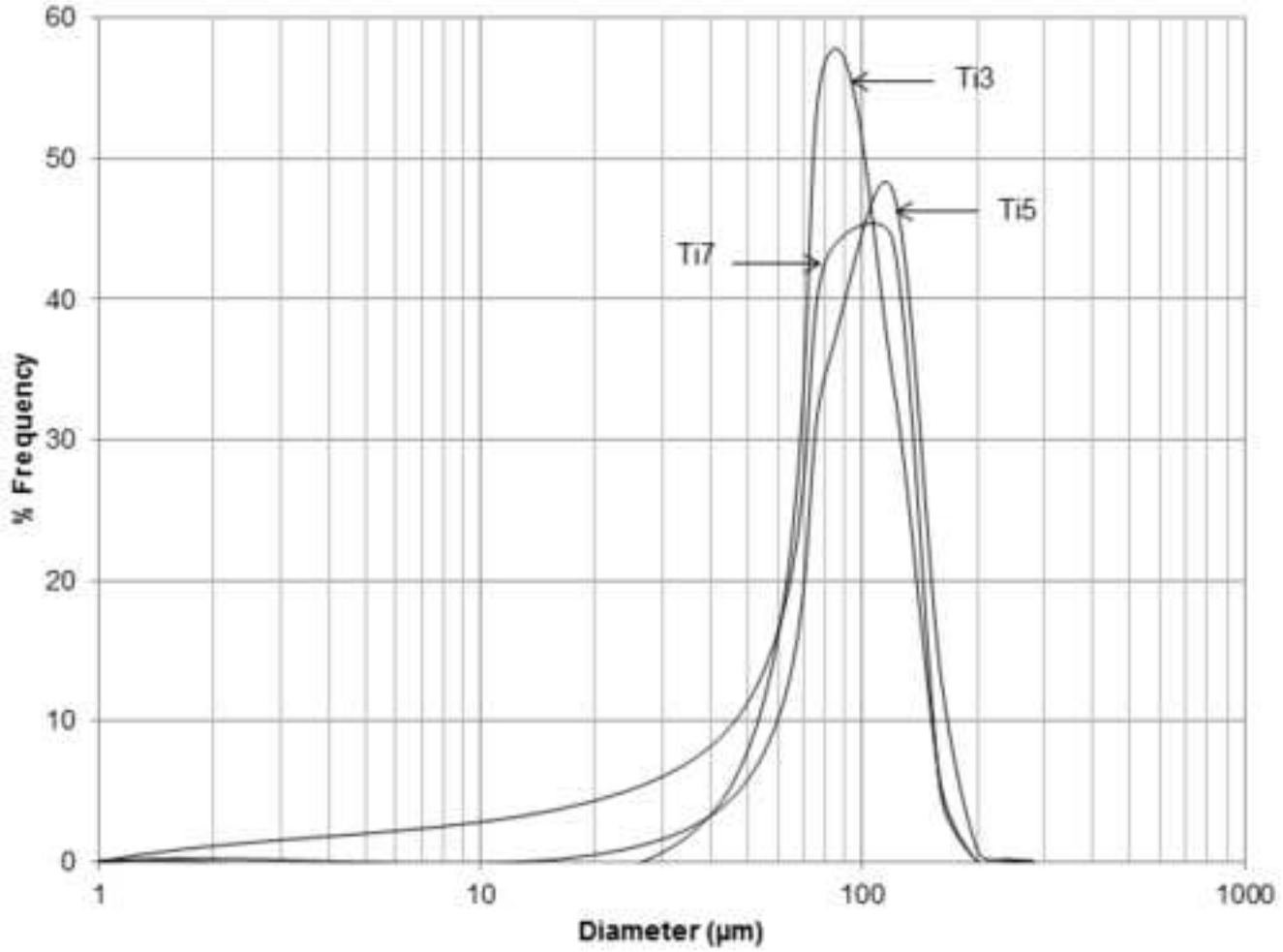

Figure 2: Particle size distribution of microspheres obtained from the investigated glass compositions

Figure 3
Click here to download high resolution image

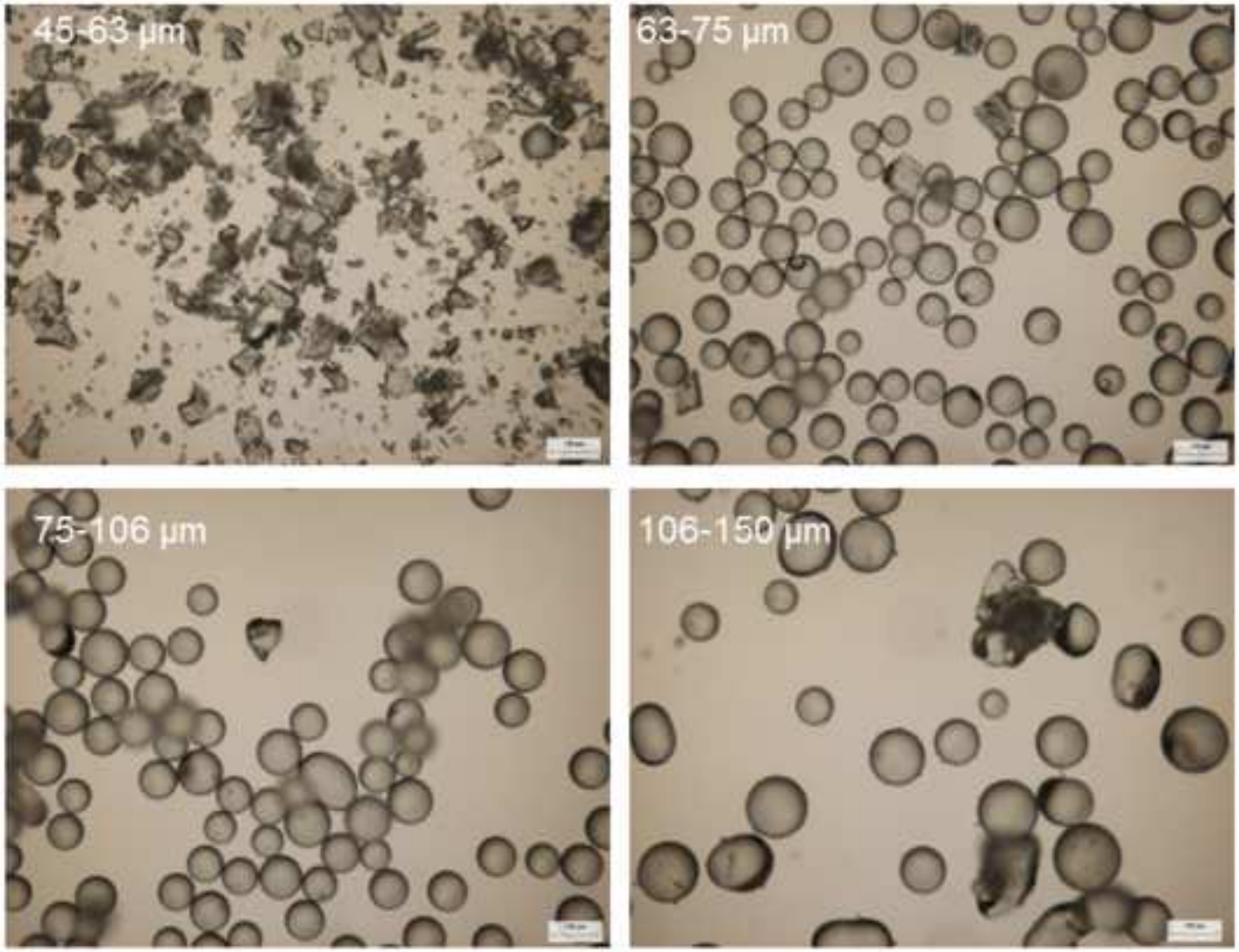

Figure 3: Light microscopy images of Ti7 microspheres for different size ranges

Figure 4

Click here to download high resolution image

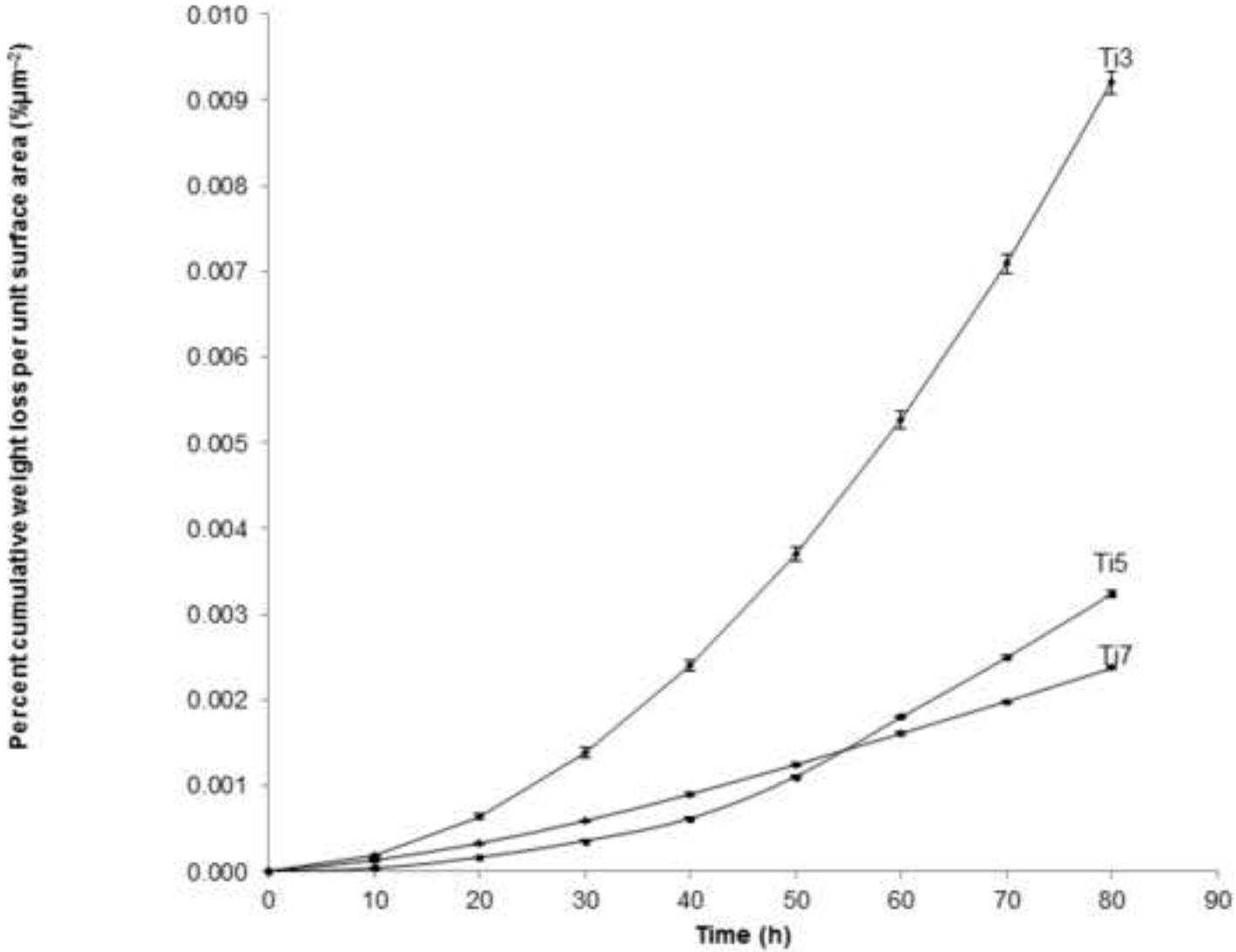

Figure 4: Degradation presented as percent cumulative weight loss per unit surface area (%µm^{-2}) as a function of time for the investigated titanium phosphate glass microspheres

Figure 5

Click here to download high resolution image

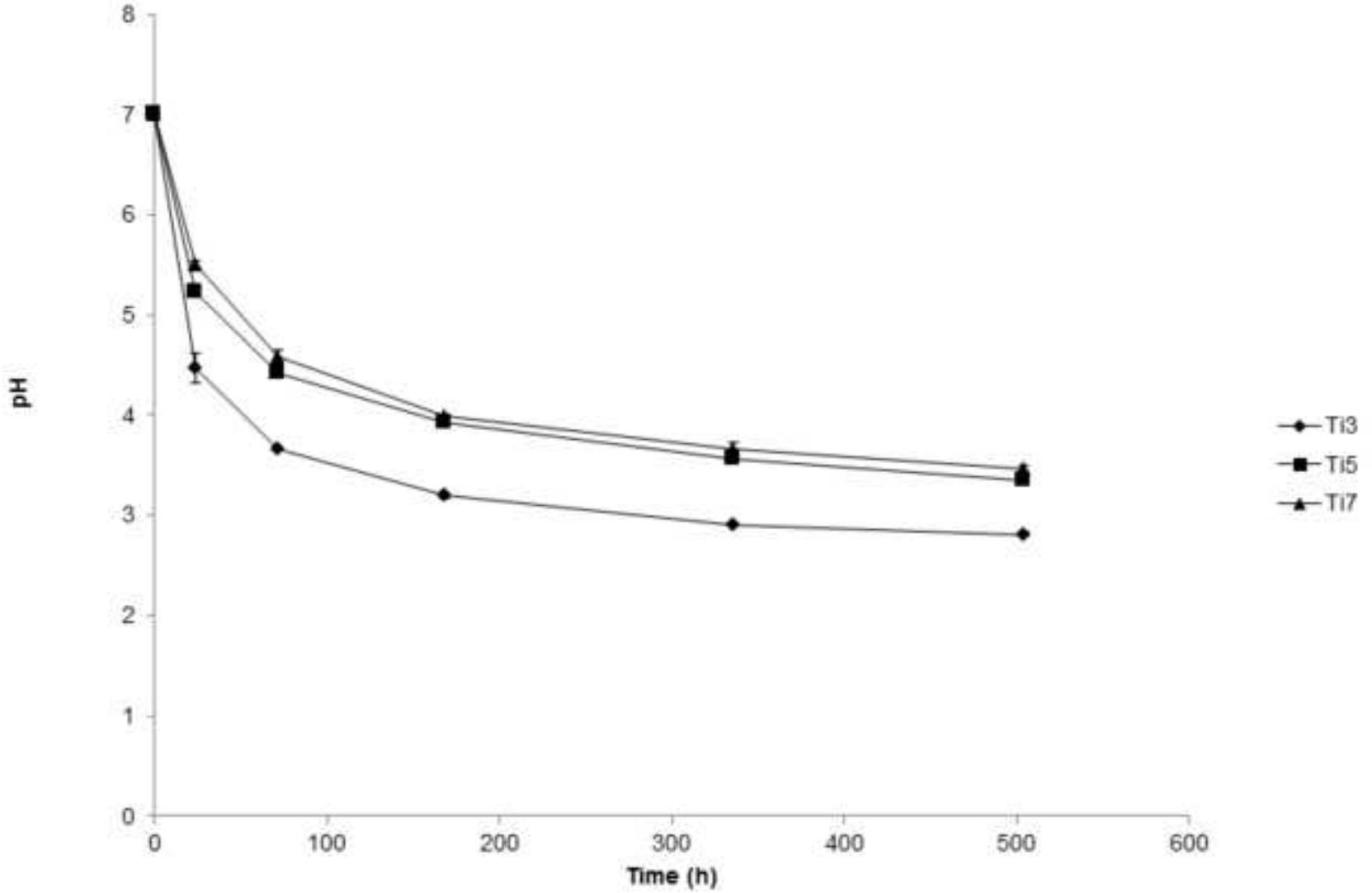

Figure 5: Variation in pH for microsphere samples immersed in deionised water as a function of time

Figure 6

Click here to download high resolution image

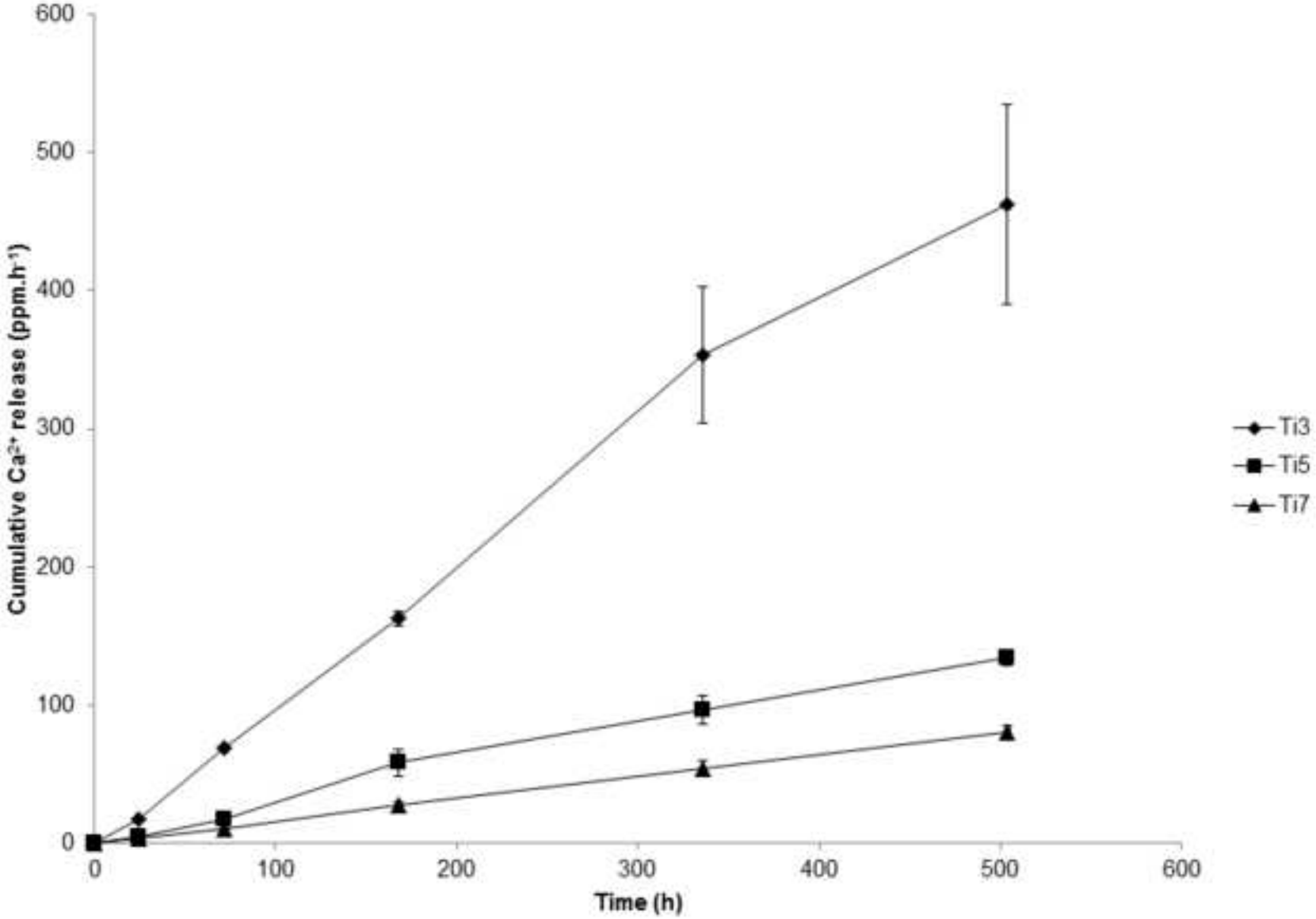

Figure 6: Cumulative release (ppm) of Ca^{2+} ions as a function of time for phosphate glass microspheres with different titanium contents

Figure 7

Click here to download high resolution image

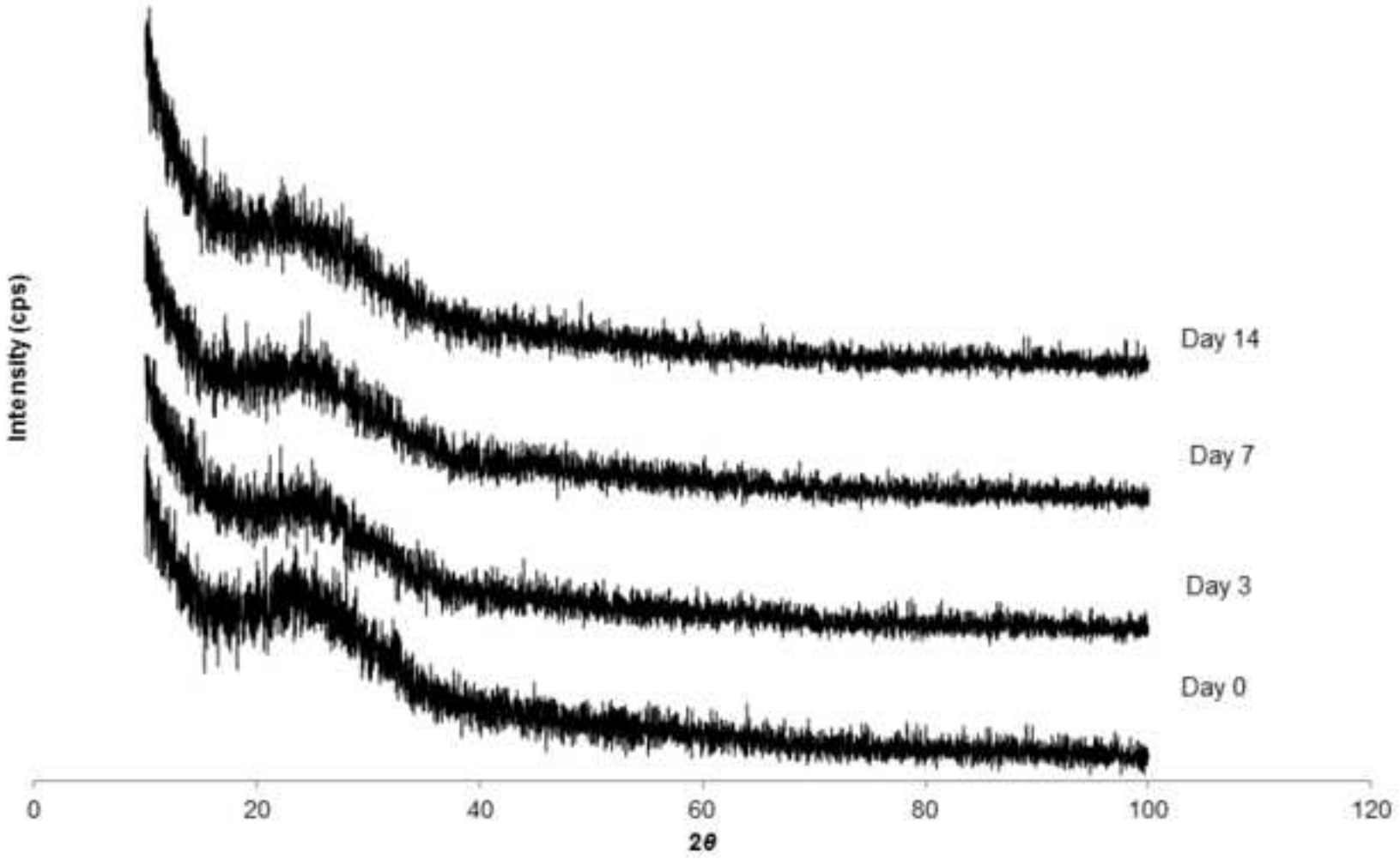

Figure 7: XRD patterns obtained for Ti5 microspheres when soaked in SBF for various periods

Figure 8

Click here to download high resolution image

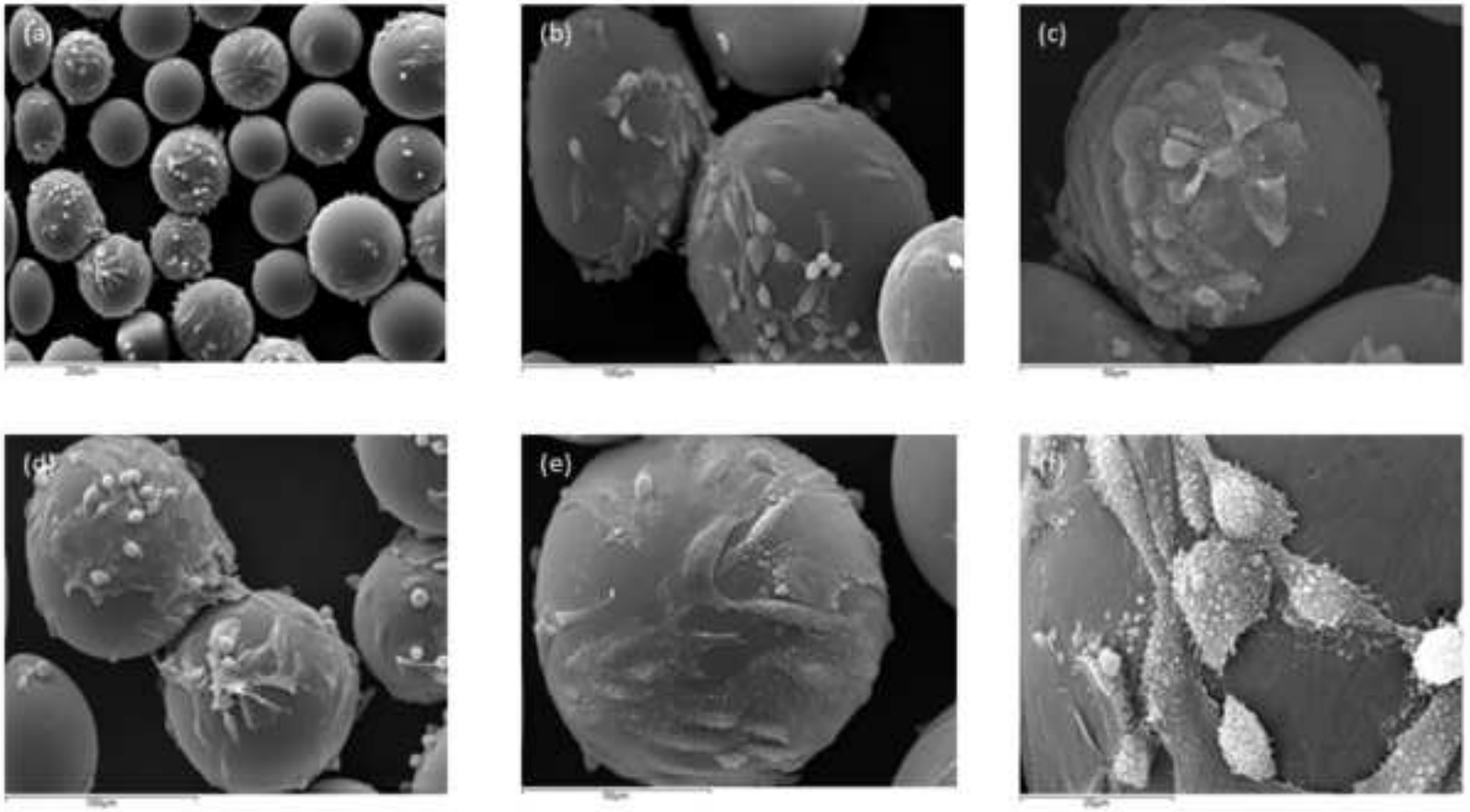

Figure 8: SEM images of titanium phosphate glass microspheres cultured with MG63 cells at day 7. (a) Ti3 microspheres; (b, c) Ti7 microspheres; (d-f) Ti5 microspheres.

Figure 9
Click here to download high resolution image

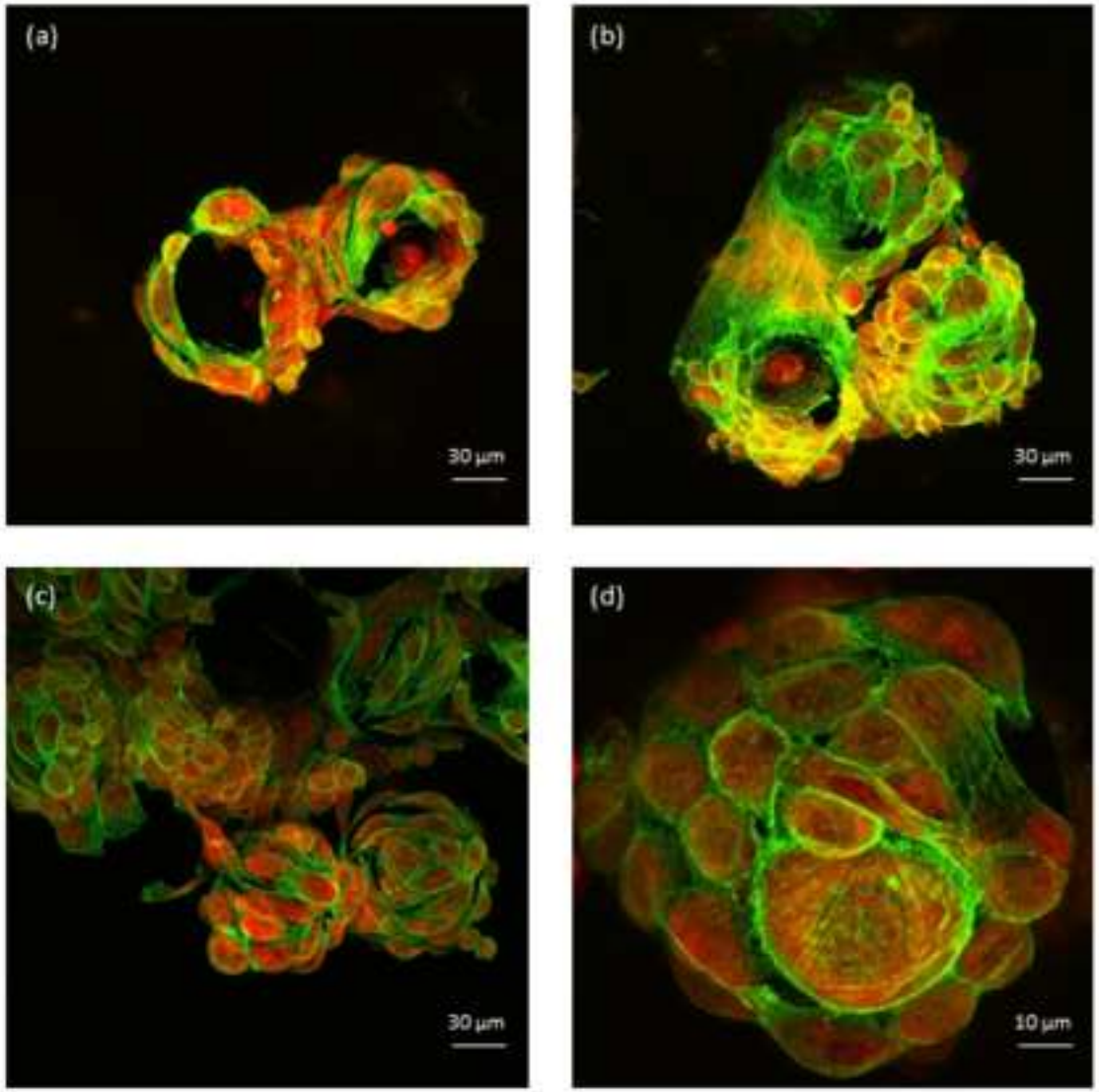

Figure 9: SLCM images of microspheres of MG63 cells attached to the investigated microspheres at 7 days post culture. (a) Ti3 microspheres, (b) Ti7 microspheres (c,d) Ti5 microspheres.

Figure 10

Click here to download high resolution image

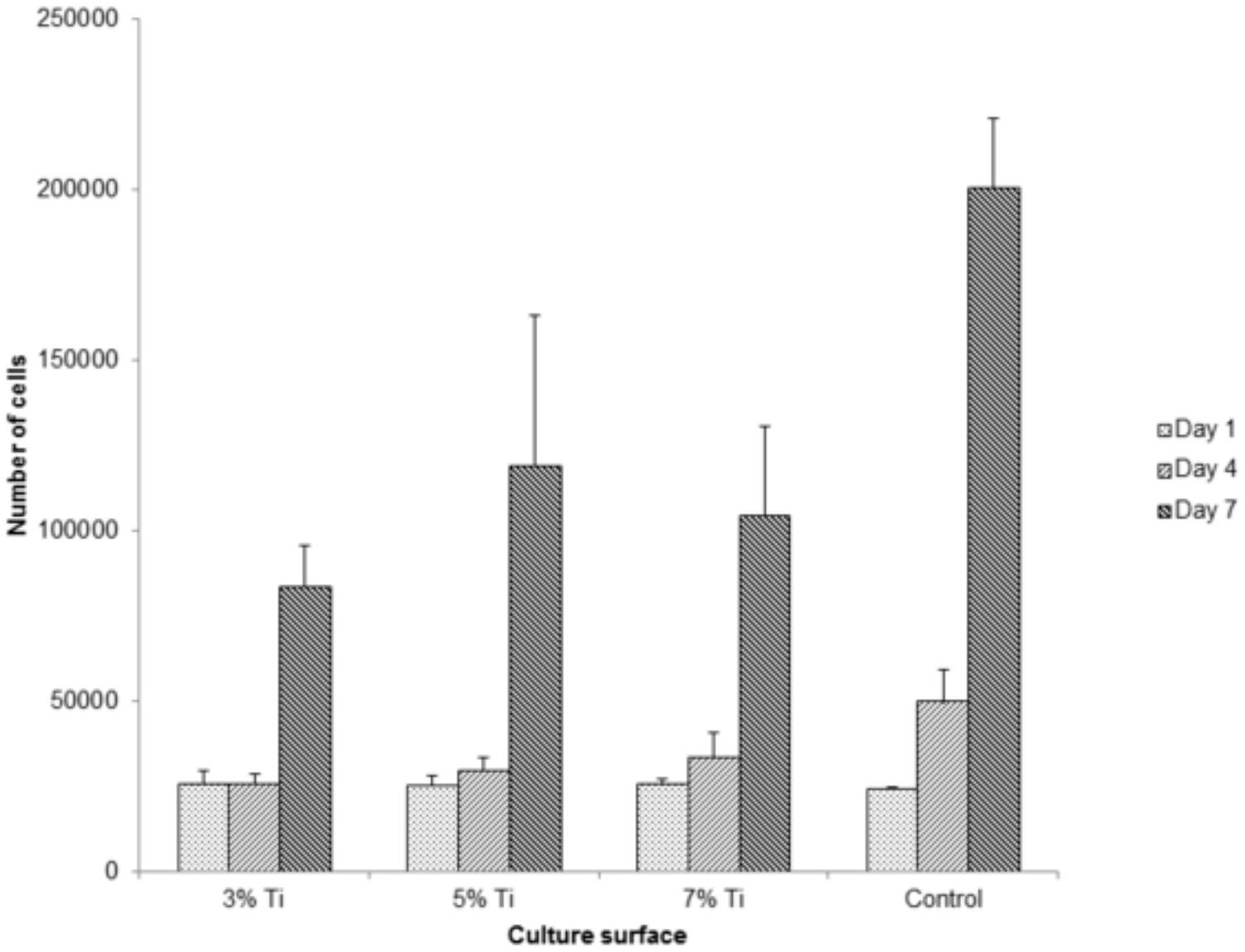

Figure 10: Results of AlamarBlue™ assay carried out for MG63 cells cultured on Ti3, Ti5 and Ti7 glass microspheres over time points of 1, 4 and 7 days.

Table 1

Click here to download high resolution image

Table 1

Glass code	Glass composition (mol%)				Melting temperature (°C)	Melting time (h)	Density (g.cm^{-3})	T_g (° C)	T_c (° C)	T_m (° C)	Q^1* chemical shift (ppm)	Q^2 chemical shift (ppm)	Q^1** (%)	Q^2 (%)
	P_2O_5	CaO	Na_2O	TiO_2										
Ti3	50	40	7	3	1300	3	2.635 ± 0.004	489	689	878	−9.4	−26.3	0.3	99.7
Ti5	50	40	5	5	1300	3	2.653 ± 0.001	510	720	904	−9.6	−26.5	0.5	99.5
Ti7	50	40	3	7	1350	5.5	2.671 ± 0.002	529	739	905	−10.1	−26.8	1.1	98.9

* Errors in Q^1 and Q^2 chemical shifts are 0.5 ppm for all compositions
** Errors in Q^1 and Q^2 percentage values are 1% for all compositions

Table 2

Click here to download high resolution image

Table 2

Glass code		Ti3	Ti5	Ti7
Anion (ppm.h^{-1})	PO_4^{3-}	37.921	5.2563	3.6023
	$P_3O_9^{3-}$	46.864	13.304	7.4739
	$P_2O_7^{4-}$	15.084	3.2237	2.2045
	$P_3O_{10}^{5-}$	18.761	8.1531	5.5788
Cation (ppm.h^{-1})	Ca^{2+}	45.778	15.202	7.462
	Na^{+}	15.571	1.9666	0.772